HHS Public Access

Author manuscript

J Struct Biol. Author manuscript; available in PMC 2016 August 01.

Published in final edited form as:

J Struct Biol. 2015 August ; 191(2): 236–244. doi:10.1016/j.jsb.2015.06.003.

Structure of EspB, a secreted substrate of the ESX-1 secretion system of *Mycobacterium tuberculosis*

Natalia Korotkova[1,†], **Jérémie Piton**[2,†], **Jonathan M. Wagner**[1,§], **Stefanie Boy-Röttger**[2], **Aleksandre Japaridze**[3], **Timothy J. Evans**[1,#], **Stewart T. Cole**[2], **Florence Pojer**[2,*], and **Konstantin V. Korotkov**[1,*]

[1]Department of Molecular & Cellular Biochemistry, and Center for Structural Biology, University of Kentucky, Lexington, Kentucky, 40536, United States of America [2] Global Health Institute, Ecole Polytechnique Fédérale de Lausanne, CH-1015 Lausanne, Switzerland [3]Laboratory of Physics of Living Matter, Ecole Polytechnique Fédérale de Lausanne, CH-1015 Lausanne, Switzerland

Abstract

Mycobacterium tuberculosis secretes multiple virulence factors during infection *via* the general Sec and Tat pathways, and *via* specialized ESX secretion systems, also referred to as type VII secretion systems. The ESX-1 secretion system is an important virulence determinant because deletion of ESX-1 leads to attenuation of *M. tuberculosis*. ESX-1 secreted protein B (EspB) contains putative PE (Pro-Glu) and PPE (Pro-Pro-Glu) domains, and a C-terminal domain, which is processed by $MycP_1$ protease during secretion. We determined the crystal structure of PE–PPE domains of EspB, which represents an all-helical, elongated molecule closely resembling the structure of the PE25–PPE41 heterodimer despite limited sequence similarity. Also, we determined the structure of full-length EspB, which does not have interpretable electron density for the C-terminal domain confirming that it is largely disordered. Comparative analysis of EspB in cell lysate and culture filtrates of *M. tuberculosis* revealed that mature secreted EspB forms oligomers. Electron microscopy analysis showed that the N-terminal fragment of EspB forms donut-shaped particles. These data provide a rationale for the future investigation of EspB's role in *M. tuberculosis* pathogenesis.

[*]Correspondence to: Florence Pojer, Ecole Polytechnique Fédérale de Lausanne, Global Health Institute, CH-1015 Lausanne, Switzerland, Phone: +41 21 69 31772, Fax: +41 21 69 31790, florence.pojer@epfl.ch, and Konstantin V. Korotkov, Department of Molecular & Cellular Biochemistry, University of Kentucky, 741 South Limestone, Lexington, KY 40536, USA, Phone: 859-323-5493, Fax: 859-257-2283, kkorotkov@uky.edu.

[†]Contributed equally.

[§]Current address: Department of Molecular Physiology and Biological Physics and The Myles H. Thaler Center for AIDS and Human Retrovirus Research, University of Virginia, Charlottesville, Virginia, United States of America

[#]Current address: Division of Regulatory Services, College of Agriculture, Food and Environment, University of Kentucky, Lexington, Kentucky, United States of America

5. Accession numbers

The coordinates and structure factors were deposited to the Protein Data Bank with accession codes 4XWP, 4XXN, 4XXX and 4XY3.

Keywords

PE domain; PPE domain; type VII secretion system; ESX

1. Introduction

Mycobacterium tuberculosis is the causative agent of tuberculosis, one of the most devastating bacterial infectious diseases worldwide. The growth and virulence of *M. tuberculosis* depends on homologous ESX secretion systems, also known as type VII secretion systems, which export a number of protein effectors across membranes to the bacterial surface and environment. *M. tuberculosis* encodes five *esx* loci, ESX-1 to ESX-5 (Cole et al., 1998), and three systems (ESX-1, ESX-3 and ESX-5) have been shown to be active in secretion (Houben et al., 2014). The number of ESX clusters varies among mycobacteria and some strains have an additional plasmid-encoded ESX-1P system (Ummels et al., 2014). The ESX-1 secretion system is critical for virulence of *M. tuberculosis* and is required for bacterial replication in macrophages, phagosomal escape into the cytosol, cellular inflammation, host-cell death, and subsequent bacterial dissemination (Guinn et al., 2004; Majlessi et al., 2005; van der Wel et al., 2007; Houben et al., 2012; Simeone et al., 2012). The ESX-3 and ESX-5 systems have been shown to be essential for *M. tuberculosis* growth (Serafini et al., 2009; Bottai et al., 2012). The ESX-3 locus is involved in zinc and iron uptake (Serafini et al., 2009; Siegrist et al., 2009; Siegrist et al., 2014). The ESX-5 system is associated with virulence mechanisms by modulating host immune responses to the mycobacteria (Abdallah et al., 2011; Bottai et al., 2012).

Two highly immunogenic proteins, EsxA (ESAT-6) and EsxB (CFP-10), are the most studied virulence factors secreted by the ESX-1 system (Stanley et al., 2003). They belong to the WxG100 family of small helical proteins that lack a canonical Sec or Tat secretion signals and form heterodimers comprised of two chains about 100 residues long (Pallen, 2002). Members of this family of secreted proteins are encoded within all known ESX gene clusters. The WxG100 family is structurally similar to two other families of ESX secreted proteins known as PE and PPE proteins. PE and PPE proteins also form a heterodimer that is likely secreted in a folded conformation (Strong et al., 2006). The majority of PE and PPE proteins contain relatively conserved N-terminal domains and C-terminal segments of variable length and sequence (Cole et al., 1998; Gey van Pittius et al., 2006). The function of PE and PPE C-terminal domains is largely unknown, although some of the PE and PPE proteins carry functional lipase and protease domains (Mishra et al., 2008; Daleke et al., 2011; Sultana et al., 2011; Sultana et al., 2013). The conserved structure of the PE–PPE N-terminal domains is important for PE–PPE heterodimer folding (Strong et al., 2006). In the structure of *M. tuberculosis* PE25–PPE41 — a heterodimer that lacks the C-terminal domains — the proteins interact via a hydrophobic interface forming a four-helix bundle with two α-helices contributed by both PE25 and PPE41 (Strong et al., 2006). Secretion of PE–PPE proteins is mediated by EspG chaperones (Daleke et al., 2012c). The structure of the PE25–PPE41–$EspG_5$ complex revealed that the EspG chaperone interacts with a relatively conserved motif on the PPE41 protein (Korotkova et al., 2014; Ekiert and Cox, 2014).

In addition to EsxA, EsxB, PE35 and PPE68, the ESX-1 system encodes Esp secreted proteins: EspA, EspB, EspC, EspE, EspJ, EspK (McLaughlin et al., 2007; Xu et al., 2007; Carlsson et al., 2009; Champion et al., 2009). The mechanism of secretion of WxG100, PE–PPE, and Esp proteins by ESX-1 secretion system is not well understood. Some Esp proteins share the highly conserved YxxxD/E secretion motif that has been identified in WxG100 and PE proteins (Daleke et al., 2012a). While this motif is required for secretion, it does not by itself determine through which ESX system the proteins are transported.

EspB, the most studied of the secreted Esp proteins, is required for host-cell death and lack of EspB secretion is associated with delays in extrapulmonary dissemination of *M. tuberculosis* in mice (Ohol et al., 2010). During translocation, a full-length 60 kDa EspB protein is cleaved within the relatively unstructured C-terminal region by $MycP_1$ protease to yield a mature 50 kDa isoform (Ohol et al., 2010). *In vitro* analysis identified residues A358 and A386 of EspB as specific cleavage sites (Wagner et al., 2013; Solomonson et al., 2013). Intriguingly, the mature EspB isoform has been predicted to include both PE- and PPE-like regions organized into a single protein chain within its N-terminal domains (Wagner et al., 2013). In contrast, the C-terminal region of EspB is glycine-rich and lacks secondary structure (Wagner et al., 2013). This observation raises two questions: (i) what is the function of the EspB mature isoform, and (ii) how does the unprocessed C-terminus affect this function.

It has been shown that EspB is required for secretion of two major ESX-1 secreted substrates, EsxA and EsxB proteins (Xu et al., 2007). Moreover, EsxA and EsxB are necessary for secretion of EspB. Thus, secretion of EspB and these WxG100 proteins is co-dependent, which suggests that EspB may interact with the EsxA and EsxB proteins. Interestingly, the C-terminal domain of EspB is necessary for co-dependent secretion suggesting that this region is involved in WxG100 protein binding (Xu et al., 2007).

Apart from EspB function in the translocation of EsxA and EsxB, secreted EspB may be involved in subversion of phospholipid-mediated host-cell signaling pathways (Chen et al., 2013). Purified mature EspB has been shown to recognize two biologically important phospholipids, phosphatidic acid and phosphatidylserine (Chen et al., 2013).

We have carried out studies to better understand the role of EspB in virulence and the mechanism for EspB secretion through the ESX secretion systems. Here, we show that mature EspB oligomerizes in the culture filtrate and forms donut-shaped ring. Our structural analysis of the full-length EspB demonstrates that the N-terminal region represents a fusion of PE and PPE proteins into a single protein with most of the hallmarks of a PE–PPE heterodimer, but lacking an EspG-binding site. The C-terminal domain of EspB is disordered in our crystal structure. Taken together, our work provides insight into the evolution of PE, PPE and EspB protein families, and their possible roles in virulence factor co-secretion.

2. Materials and methods

2.1. Culture supernatant and cell lysate preparation, and immunoblotting analysis of EspB

M. tuberculosis Erdman strain espA::Tn-pMDespACD was grown in 7H9 complete broth to late-logarithmic phase (OD_{600} ~0.8–1) of growth (Chen et al., 2012). These cells were subcultured into Sauton's liquid medium, supplemented with 0.05% Tween-80, at starting OD_{600} of 0.05. Cells were grown to mid-logarithmic phase of growth (OD_{600} of 0.6–0.7), centrifuged, washed twice with PBS, resuspended in Sauton's medium without Tween-80 and incubated further for several more days. Cultures were harvested by centrifugation to yield the cell pellet and culture supernatant. The culture supernatant was filtered sequentially through 0.2 and 0.4 micron filters and concentrated in Vivaspin columns with 5-kDa molecular weight cut-off membranes (Sartorius Stedim Biotech GmbH, Goettingen, Germany) prior to analyses. Cell lysates were prepared by resuspending cell pellets in lysis buffer (Phosphate Buffered Saline with 0.1% Triton X-100, 10% glycerol and Roche protease inhibitor cocktail tablets), bead beating with 100 micron glass beads, and clarifying by centrifugation. Total protein concentration in all preparations was determined using BCA assays with bovine serum albumin as the standard.

For immunoblot analysis, 5 μg, 10 μg or 15 μg of total protein from concentrated culture supernatants or cell lysates were resolved on a NuPAGE 4 to 12% Bis-Tris gel and transferred onto a nitrocellulose membrane. The membrane was blocked with TBS-Milk (20 mM Tris-HCl, pH 7.5, 500 mM NaCl and 5% non-fat milk powder) and incubated overnight with anti-EspB rat polyclonal antibody diluted in TNT-BSA (20 mM Tris-HCl, pH 7.5, 500 mM NaCl, 0.05% Tween-20 and 1% BSA fraction V) at 4°C (Chen et al., 2013). The membrane was washed with TNT, incubated with appropriate secondary antibody in TNT-BSA for 30 min at room temperature and developed using Lumi-Light Plus chemiluminescence reagent (Roche, Mannheim, Germany).

2.2. Cloning, expression and purification of EspB

The full-length protein $EspB_{1\text{-}460}$ was purified as described (Wagner et al., 2013). For crystallization studies, a shorter construct was designed to encompass PE and PPE domains of EspB (residues 7–278) and cloned into a modified pET-28b vector (EMD Millipore) with an N-terminal His_6-tag and a TEV protease cleavage site. A 600-mL culture (LB) of *Escherichia coli* strain Rosetta2(DE3) carrying $EspB_{7\text{-}278}$-encoding plasmid was grown to an OD_{600} of 0.6 at 37°C and $EspB_{7\text{-}278}$ expression was induced by the addition of 0.5 mM isopropylthio-β-galactoside (IPTG) at 24°C. The culture was harvested after 4 h, pelleted, and frozen at −80 °C until further use. The pull-down experiments with EspB and $EspG_1$ were performed as described (Korotkova et al., 2014).

The frozen cells were resuspended in 20 mM Tris pH 8.5, 300 mM NaCl, 10 mM imidazole at 4 °C. The suspension was passed five times through a cell disrupter and the lysate centrifuged for 45 min at 17,000 × g. The resultant suspension was applied to a 5-mL Ni-NTA column pre equilibrated with the lysis buffer. The resin was then washed with 20 mM Tris pH 8.5, 300 mM NaCl, 20 mM imidazole and $EspB_{7\text{-}278}$ was eluted in a gradient with a buffer containing 250 mM imidazole. Fractions were analyzed by SDS-PAGE, and fractions

with $EspB_{278}$ were pooled, concentrated around 10 mg/mL and dialyssed overnight at 4°C in 20 mM HEPES pH 7.5, 300 mM NaCl and TEV protease. Cleaved protein solution was injected on a size-exclusion chromatography column Superdex200 16/30 pre-equilibrated with 20 mM HEPES pH 7.5, 100 mM NaCl. Fractions containing $EspB_{7\text{-}278}$ were isolated and pooled, and protein was concentrated to 10 mg/mL. Protein purity was verified and estimated at >90%.

For the electron microscopy analysis, the N-terminal EspB fragment (residues 1-338) was cloned into pHis9gw vector (O'Maille et al., 2004). The resulting plasmid, allowing expression of an EspB N-terminal fusion with a His-tag, was transformed into *E. coli* BL21 (DE3) cells. Protein expression was induced at OD_{600}=0.6 with 0.5 mM IPTG overnight at 16°C. His_6-tagged protein was purified with a Ni-NTA column similar to $EspB_{7\text{-}278}$.

2.3. Crystallization and data collection

Crystals of full-length $EspB_{1\text{-}460}$ were obtained by hanging drop vapor diffusion using 0.1M CAPSO pH 10.8, 0.2M sodium chloride, 1.5M ammonium sulfate. Crystals of $EspB_{7\text{-}278}$ were grown by hanging drop vapor diffusion in 0.2M calcium acetate, 0.1M Tris-HCl, 20% PEG3000 (space group $C222_1$) and 0.2M sodium chloride, 0.1M CAPS pH 10.5, 1.26M ammonium sulfate (space group *I*222). Data were collected at Southeast Regional Collaborative Access Team (SER-CAT) 22-ID beamline at the Advanced Photon Source, Argonne National Laboratory. All data were processed and scaled using *XDS* and *XSCALE* (Kabsch, 2010).

To obtain the crystal structure of $EspB_{7\text{-}278}$ in complex with phospholipids, preliminary crystallization trials were performed at 291° K by sitting drop vapor diffusion and manually optimized by vapor diffusion in hanging drops containing 1 μL of reservoir solution and 1 μL of protein. $EspB_{7\text{-}278}$ crystallized at 10 mg/mL in multiple conditions and the best crystals of $EspB_{7\text{-}278}$ were grown in 0.2 M potassium dihydrogen phosphate, 20% w/v PEG3350 with 1 mM L-α-phosphatidylserine (Avanti Polar Lipids, Inc) as an additive in the mixed drop. Crystals were cryoprotected in reservoir mother liquor supplemented with 25% glycerol and directly flash cooled in liquid nitrogen. Diffraction data were collected on PXIII of the Swiss Light Source (SLS, PSI, Villigen, Switzerland). All data were integrated with the program *XDS* (Kabsch, 2010) and processed using the CCP4 program suite (Collaborative Computational Project, 1994).

2.5. Structure determination and refinement

The structure of $EspB_{7\text{-}278}$ in space group $C222_1$ was solved by molecular replacement using Phaser (McCoy et al., 2007) and the structure of PE25–PPE41 heterodimer (PDB: 2G38) (Strong et al., 2006) converted to a poly-Ala search model. After electron density modification using Parrot (Zhang et al., 1997), a preliminary model was built using Buccaneer (Cowtan, 2006). The model was corrected in Coot (Emsley et al., 2010) and expanded using ARP/wARP (Langer et al., 2008). The structure was refined to 1.82 Å resolution with R_{work} 0.199 and R_{free} 0.234 using REFMAC5 (Murshudov et al., 2011). The final model (PDB: 4XWP) includes residues 7–278 of EspB with the loop residues 86–115 and 125–130 missing due to disorder.

The structure of $EspB_{7-278}$ in space group *I*222 was solved by molecular replacement using Phaser and structure of $EspB_{7-278}$ in space group $C222_1$ (PDB: 4XWP). The structure was corrected in Coot and refined to 2.14 Å resolution with R_{work} 0.204 and R_{free} 0.251 using REFMAC5. The loop residues 82–114 are missing in this structure.

The best crystal of $EspB_{7-278}$ grown in the presence of phosphatidylserine diffracted to 1.5 Å and belonged to the same $C222_1$ space group as the original apo-$EspB_{7-278}$. This model was subjected to iterative rounds of re-building and refinement in Coot and REFMAC5. The structure was refined to 1.5 Å resolution with R_{work} 0.194 and R_{free} 0.218 using REFMAC5 and applying seven translation, libration and screw-rotation displacement (TLS) groups determined by the TLSMD server (Painter and Merritt, 2006). No electron density that could be attributed to phosphatidylserine was found. This structure has less disordered segments than the isomorphous $EspB_{7-278}$ structure (PDB: 4XWP) with only residues 90–114 missing, and there are some differences in crystal contacts due to the distinctive composition of crystallization solutions.

Structure of $EspB_{1-460}$ was solved by molecular replacement using Phaser and $EspB_{7-278}$ structure (PDB: 4XXN). The model was re-built and extended in Coot and refined with phenix.refine (Afonine et al., 2012) and REFMAC5. The final model was refined to 3.04 Å resolution with R_{work} 0.220 and R_{free} 0.266 The C-terminal domain is disordered in this structure and only 5 additional C-terminal residues 279–283 were added to the model compared to the truncated $EspB_{7-278}$ structure. The quality of structures was assessed using Coot and the MolProbity server (Chen et al., 2010). The structural figures were generated using PyMol (www.pymol.org).

2.6. Negative staining electron microscopy

Proteins samples (15 µl at 0.01 mg/mL, in 25 mM Tris-HCl pH 7.5 and 150 mM NaCl) were pipetted on the carbon-coated grid (400 mesh copper Grids, Canemco-Marivac) for 3 min, the grid was washed with distilled water, and further treated with uranyl acetate aqueous solution (15 µL, 2% (w/v) for 30 s. Grids were imaged on a Tecnai Spirit microscope at 80 kV.

3. Results

3.1. Secreted EspB forms oligomers

EspB is expressed by *M. tuberculosis* as a full-length 60 kDa precursor protein and secreted by the ESX-1 secretion system after the cleavage of the C-terminal domain, by the serine protease $MycP_1$, as a mature 50 kDa isoform (Fig. 1A). It has been reported that EspB is predominantly present as the 50 kDa isoform in *M. tuberculosis* culture filtrate (McLaughlin et al., 2007; Ohol et al., 2010). In order to analyze the oligomeric state of EspB, we performed immunoblotting experiments on proteins from cell lysate and culture filtrate after electrophoresis on a native gel. Intriguingly, we observed that EspB is in a higher oligomeric state in the culture filtrate than in the cell lysate (Fig. 2B). Despite several efforts we were not able to increase the resolution on the native gel to determine the size of the complex by this method, nor could we further analysis the identities of the bands by mass spectrometry

methods due to low material level. In order to examine further the oligomeric state of EspB, we overexpressed in *E. coli* and purified the N-terminal domain of EspB, $EspB_{1-338}$ (Chen et al., 2013; Ohol et al., 2010). Size exclusion chromatography revealed a mix between two species, a monomeric EspB state, and a higher oligomeric state. This observation was confirmed by the immunoblotting experiments on the native gel (Fig. 1B).

In order to determine if this oligomer was organized in a specific structure, negative staining electron microscopy was performed on a sample corresponding to the top of the peak of the oligomer form of $EspB_{1-338}$ (Fig. 1C). Surprisingly, we observed a homogeneous sample with small particles of an approximate size of 10 × 10 μm with a donut ring shape (Fig. 1D). Unfortunately, only one preferential orientation of the particle was observed that did not allow a high-resolution structural study.

3.2. Structure of EspB

In order to gain insight into the EspB structure we expressed in *E. coli* and purified a full-length protein, $EspB_{1-460}$. Crystals of the full-length protein were obtained but diffracted to a limited resolution ~3.0 Å and experimental phasing was unsuccessful thus precluding structure determination. Therefore, we expressed and purified a shorter EspB construct for structural studies, $EspB_{7-278}$, that contains only the predicted PE-PPE domains and lacks the C-terminal disordered region. $EspB_{7-278}$ crystallized in multiple conditions in two different crystal forms (Table 1). The best 1.5 Å resolution dataset was obtained from crystals belonging to the space group $C222_1$ that were grown in the presence of phosphatidylserine but no lipid was found in the structure. The structure $EspB_{7-278}$ was solved by molecular replacement using the structure of the PE25–PPE41 heterodimer (PDB: 2G38) as a search model (Strong et al., 2006). There is one monomer per asymmetric unit in both crystal forms. Structures of $EspB_{7-278}$ superimpose with r.m.s.d. of 0.33–1.12 Å between Cα atoms with the largest differences found in the loop regions (Fig. 2). Next, the structure of full-length $EspB_{1-460}$ was solved using our $EspB_{7-278}$ structure as a search model. However, the C-terminal region of $EspB_{1-460}$ was disordered in the structure. Analyzing the crystal content of those different high-resolution structures of EspB, did not indicate any donut shape ring oligomers in the way the molecules are packing, as observed in the EM studies described above.

3.3. Comparison of EspB and PE25–PPE41 heterodimer structure

EspB structures showed that the N-terminal domain of EspB contains alpha helical elements arranged in a paperclip-like structure very similar to that observed for the PE25–PPE41 heterodimer (Fig. 3A). Indeed, EspB is structurally similar to the PE25–PPE41 heterodimer and is superimposable with an r.m.s.d. of 1.9 Å over 249 Cα atoms and 17% sequence identity (Fig. 3B). EspB contains 7 alpha helices in its N-terminal domain. The first two helices (residues 10–21 and residues 39–89, respectively) correspond to helices α1 and α2 of PE25 and adopt an antiparallel hairpin. Helix α1 of EspB is significantly shorter than helix α1 of PE25, 11 versus 30 residues. As a result, the α1–α2 loop of EspB is longer and adopts an extended conformation. Proline residues P28, P29, P33 and P36 act as ‘knobs-in-the-holes’ in the groove between helices α2 and α4. This α1–α2 loop is not conserved in mycobacterial EspB homologs (Supplementary Fig. S1).

Residues 90–132 of EspB comprise a partially unstructured linker region that is absent in PE–PPE heterodimers. The linker serves to connect helix α2 of PE domain of EspB to helix α3 of the PPE domain of EspB, which corresponds to helix α1 of PPE41. This linker region does not associate tightly with the rest of the protein and residues 89–115 are disordered in all crystal forms. Residues 116–124 contact helix α2 and helix α7 and are well ordered (Fig. 2C and 2D). The loop residues 125–130 display flexibility and are either disordered or adopt different conformations (Fig. 2C and 2D). The WxG motif of EspB (residues 176–178) is positioned at the beginning of helix α5 where W176 contributes to a tight interface between helices α2 and α5 (Fig. 3A). This is analogous to the interaction mediated by W56 of PPE41. However, the position of the indol moieties of $W176_{EspB}$ and $W56_{PPE41}$ differs in the EspB and PE25–PPE41 structures. While $W56_{PPE41}$ makes van der Waals contacts with $Y87_{PE25}$ in the PE25–PPE41 structure, $W176_{EspB}$ is positioned deeper, between helices α2 and α5, and the Nε atom of $W176_{EspB}$ forms a hydrogen bond with the hydroxyl group of $Y81_{EspB}$ (Figs 3A and 4A). The PE and PPE sequence motifs are not conserved in EspB and residues QQ (11–12) and DLK (132–134) replace PE and PPE, respectively (Fig. 3B). Interestingly, EspB is missing about 9 residues compared to the α4–α5 loop region of PPE41. This means that EspB is about 11Å shorter than PE25–PPE41 at one end and it lacks many of the key residues involved in the PPE41–$EspG_5$ interface including residues D121–T129 that contain the characteristic hh motif of PPE proteins (Fig. 3A and Supplementary Fig. S2). Furthermore, while the length and sequence of the α4–α5 loop of PPE proteins are conserved (Korotkova et al., 2014; Ekiert and Cox, 2014), the corresponding region in the EspB homologs displays both length and sequence variability (Supplementary Fig. S1). To confirm that EspB does not recognize the ESX-1-specific chaperone $EspG_1$, *M. tuberculosis* $EspG_1$ was expressed in *E. coli* and employed for pull-down experiments with both full-length and mature isoforms of EspB. The analysis did not detect EspB binding to $EspG_1$. Thus, EspB has evolved as a fusion of PE and PPE proteins, which seemingly lost its requirement of EspG for folding/stability.

Although full-length $EspB_{1\text{-}460}$ (PDB: 4XY3) was crystallized, residues in the C-terminal region beyond K283 could not be modeled. The remaining 177 residues are presumably present in an unstructured form extending from the top of the groove formed by helices α1 and α5.

3.3. Secretion motif YxxxD/E of EspB is in a helical conformation

The conserved YxxxD/E secretion motif has been identified in a subset of secreted ESX substrates, including EsxB homologs, PE proteins and several Esp proteins (Daleke et al., 2012a). Subsequent analysis of the WxG100 protein family revealed an extended sequence pattern *H*xxxD/Exx*h*xxx*H*, where *H* is a highly conserved hydrophobic residue and *h* is a less conserved hydrophobic residue (Poulsen et al., 2014). In EspB structures the YxxxD/E sequence (residues 81–85) is located adjacent to the partially disordered PE–PPE loop. However, this segment clearly adopts a helical conformation in the high-resolution structure of $EspB_{7\text{-}278}$ (Fig. 4A). While this C-terminal segment is flexible in the NMR structures of WxG100 proteins (Renshaw et al., 2005; Ilghari et al., 2011), it adopts a helical conformation in a number of crystal structures, including *M. smegmatis* EsxG–EsxH (PDB: 3Q4H), *M. tuberculosis* EsxO–EsxP (PDB: 3OGI and 4GZR) and *M. tuberculosis* EsxA–

EsxB (PDB: 3FAV) (Arbing et al., 2013; Poulsen et al., 2014). Likewise, the YxxxD/E motif of PE25 is in a helical conformation in the PE25–PP41–$EspG_5$ structures (PDB: 4KXR and 4W4L) (Korotkova et al., 2014; Ekiert and Cox, 2014), although it is partially disordered in the structures of the PE25–PPE41 heterodimer (PDB: 2G38 and 4W4K) (Strong et al., 2006; Ekiert and Cox, 2014). What role the apparent helical nature of YxxxD/E motif in ESX substrates plays in the ESX secretion mechanism is yet to be established.

3.4. Putative lipid-binding sites of EspB

Although we have not yet been able to obtain a structure of EspB in complex with phosphatidylserine, an inspection of the EspB structure revealed the presence of several hydrophobic grooves with adjacent positive charges that may represent the lipid-binding sites (Fig. 4B). The first hydrophobic groove is located between helices α1 and α2 with residues L60, F159, L163 lining the bottom of the groove. The volume of this groove is 395 $Å^3$ as calculated by CAVER software (Chovancova et al., 2012). The second hydrophobic groove (53 $Å^3$) is located at the 'tip' of EspB structure between helices α6 and α7. Here L232 and I246 are located at the bottom, and Y236 and Y250 at the rim of the groove. The rest of EspB surface has a mixed distribution of positively and negatively charged patches (Fig. 4B), which functions remain to be determined.

4. Discussion

EspB is an essential component of the ESX-1 secretion system of *M. tuberculosis* but of poorly defined function. In this work we provide a detailed structural characterization of EspB. We show that the mature isoform of EspB is a fusion of PE and PPE N-terminal regions. Thus, all ESX secreted substrates that have been identified so far have a similar structural fold. Remarkably, the EspB protein structure lacks a chaperone-binding domain, which is conserved in PPE proteins (Korotkova et al., 2014; Ekiert and Cox, 2014). Moreover, EspB does not bind the ESX-1-specific chaperone, $EspG_1$. EspG chaperones have been implicated in the folding/stability of PE–PPE heterodimers and targeting to the cognate ESX machinery (Daleke et al., 2012c; Korotkova et al., 2014). It is unclear as to how EspB is recognized and secreted via the ESX-1 system. However, EspB has been shown to interact with EspK, which in turn interacts directly with the large, membrane-associated ATPase $EccC_{1a}$–$EccC_{1b}$ (McLaughlin et al., 2007).

The C-terminal domain of EspB is not structured in our crystal forms. Analysis of the unprocessed full-length and mature forms of EspB demonstrated that mature EspB is an oligomer in *M. tuberculosis* culture filtrate. In contrast, the full-length protein detected in the cell lysate does not oligomerize. These data suggest that the unfolded C-terminal domain of EspB could be implicated in preventing the self-association of EspB in the cytosol. Further studies should be envisaged to understand the role of the C-terminal domain in the prevention of the oligomerization of EspB. Intriguingly, like EspB, PE–PPE heterodimers are prone to oligomerization, but EspG chaperones protect the hydrophobic region on PPE thus preventing PE–PPE heterodimers from self-polymerization (Korotkova et al., 2014). It is possible that after being exported, the aggregation-prone PE–PPE proteins are stabilized

by interacting with other PE–PPE dimers similar to EspB. Further experiments are required to test this hypothesis.

$MycP_1$ protease is involved in the processing of EspB *in vivo* and *in vitro* (Ohol et al., 2010; Wagner et al., 2013; Solomonson et al., 2013). The cleavage sites are located within the unstructured C-terminal domain of EspB. $MycP_1$ belongs to the mycosin family of membrane-anchored serine proteases. MycP paralogs are present in all ESX clusters and this enzyme is essential for the ESX-1, ESX-3 and ESX-5 secretory processes. This raises the question as to what other secreted proteins might be substrates for other MycP paralogs because ESX-2, ESX-3, ESX-4 and ESX-5 clusters do not encode an obvious EspB homolog. However, all ESX clusters except ESX-4 encode *pe* and *ppe* genes. It is possible that the other MycP proteases target C-terminal domains of PE–PPE proteins. Additional studies to address this hypothesis are warranted. In conclusion, this study provides a better understanding of ESX-specific substrates and lays the groundwork for characterization of EspB and $MycP_1$ functions in the context of ESX secretion. While this manuscript was under review, Solomonson *et al.* reported crystal structure of *Mycobacterium smegmatis* EspB homolog (Solomonson et al., 2015). The structures of *M. tuberculosis* and *M. smegmatis* EspB display the same fold (2.1–2.3 Å r.m.s.d. and 28% sequence identity) but deviate in the conformation of α6–α7 helical ‘tip’ and other details.

Supplementary Material

Refer to Web version on PubMed Central for supplementary material.

Acknowledgements

Authors thank staff members of Southeast Regional Collaborative Access Team (SER-CAT) at the Advanced Photon Source, Argonne National Laboratory, for assistance during data collection. Use of the Advanced Photon Source was supported by the U. S. Department of Energy, Office of Science, Office of Basic Energy Sciences, under Contract No. W-31-109-Eng-38. We acknowledge the University of Kentucky Protein Analytical Core that is supported by NIH/NIGMS grant P30GM110787. This study was supported in part by NIH/NIGMS grant P20GM103486 to KVK. This study received funding from the Swiss National Science Foundation (31003A-140778).

References

Abdallah AM, Bestebroer J, Savage ND, de Punder K, van Zon M, Wilson L, Korbee CJ, van der Sar AM, Ottenhoff TH, van der Wel NN, Bitter W, Peters PJ. Mycobacterial secretion systems ESX-1 and ESX-5 play distinct roles in host cell death and inflammasome activation. J Immunol. 2011; 187:4744–4753. [PubMed: 21957139]

Afonine PV, Grosse-Kunstleve RW, Echols N, Headd JJ, Moriarty NW, Mustyakimov M, Terwilliger TC, Urzhumtsev A, Zwart PH, Adams PD. Towards automated crystallographic structure refinement with phenix.refine. Acta Crystallogr D Biol Crystallogr. 2012; 68:352–367. [PubMed: 22505256]

Arbing MA, Chan S, Harris L, Kuo E, Zhou TT, Ahn CJ, Nguyen L, He Q, Lu J, Menchavez PT, Shin A, Holton T, Sawaya MR, Cascio D, Eisenberg D. Heterologous expression of mycobacterial Esx complexes in Escherichia coli for structural studies is facilitated by the use of maltose binding protein fusions. PLoS One. 2013; 8:e81753. [PubMed: 24312350]

Bottai D, Di Luca M, Majlessi L, Frigui W, Simeone R, Sayes F, Bitter W, Brennan MJ, Leclerc C, Batoni G, Campa M, Brosch R, Esin S. Disruption of the ESX-5 system of *Mycobacterium tuberculosis* causes loss of PPE protein secretion, reduction of cell wall integrity and strong attenuation. Mol Microbiol. 2012; 83:1195–1209. [PubMed: 22340629]

Carlsson F, Joshi SA, Rangell L, Brown EJ. Polar localization of virulence-related Esx-1 secretion in mycobacteria. PLoS Pathog. 2009; 5:e1000285. [PubMed: 19180234]

Champion PA, Champion MM, Manzanillo P, Cox JS. ESX-1 secreted virulence factors are recognized by multiple cytosolic AAA ATPases in pathogenic mycobacteria. Mol Microbiol. 2009; 73:950–962. [PubMed: 19682254]

Chen JM, Zhang M, Rybniker J, Boy-Rottger S, Dhar N, Pojer F, Cole ST. Mycobacterium tuberculosis EspB binds phospholipids and mediates EsxA-independent virulence. Mol Microbiol. 2013; 89:1154–1166. [PubMed: 23869560]

Chen JM, Boy-Rottger S, Dhar N, Sweeney N, Buxton RS, Pojer F, Rosenkrands I, Cole ST. EspD is critical for the virulence-mediating ESX-1 secretion system in Mycobacterium tuberculosis. J Bacteriol. 2012; 194:884–893. [PubMed: 22155774]

Chen VB, Arendall WB 3rd, Headd JJ, Keedy DA, Immormino RM, Kapral GJ, Murray LW, Richardson JS, Richardson DC. MolProbity: all-atom structure validation for macromolecular crystallography. Acta Crystallogr D Biol Crystallogr. 2010; 66:12–21. [PubMed: 20057044]

Chovancova E, Pavelka A, Benes P, Strnad O, Brezovsky J, Kozlikova B, Gora A, Sustr V, Klvana M, Medek P, Biedermannova L, Sochor J, Damborsky J. CAVER 3.0: a tool for the analysis of transport pathways in dynamic protein structures. PLoS computational biology. 2012; 8:e1002708. [PubMed: 23093919]

Cole ST, Brosch R, Parkhill J, Garnier T, Churcher C, Harris D, Gordon SV, Eiglmeier K, Gas S, Barry CE 3rd, Tekaia F, Badcock K, Basham D, Brown D, Chillingworth T, Connor R, Davies R, Devlin K, Feltwell T, Gentles S, Hamlin N, Holroyd S, Hornsby T, Jagels K, Krogh A, McLean J, Moule S, Murphy L, Oliver K, Osborne J, Quail MA, Rajandream MA, Rogers J, Rutter S, Seeger K, Skelton J, Squares R, Squares S, Sulston JE, Taylor K, Whitehead S, Barrell BG. Deciphering the biology of *Mycobacterium tuberculosis* from the complete genome sequence. Nature. 1998; 393:537–544. [PubMed: 9634230]

Collaborative Computational Project, N. The CCP4 suite: programs for protein crystallography. Acta Crystallogr D Biol Crystallogr. 1994; 50:760–763. [PubMed: 15299374]

Cowtan K. The Buccaneer software for automated model building. 1. Tracing protein chains. Acta Crystallogr D Biol Crystallogr. 2006; 62:1002–1011. [PubMed: 16929101]

Daleke MH, Ummels R, Bawono P, Heringa J, Vandenbroucke-Grauls CM, Luirink J, Bitter W. General secretion signal for the mycobacterial type VII secretion pathway. Proc Natl Acad Sci U S A. 2012a; 109:11342–11347. [PubMed: 22733768]

Daleke MH, Cascioferro A, de Punder K, Ummels R, Abdallah AM, van der Wel N, Peters PJ, Luirink J, Manganelli R, Bitter W. Conserved Pro-Glu (PE) and Pro-Pro-Glu (PPE) protein domains target LipY lipases of pathogenic mycobacteria to the cell surface via the ESX-5 pathway. J Biol Chem. 2011; 286:19024–19034. [PubMed: 21471225]

Daleke MH, van der Woude AD, Parret AH, Ummels R, de Groot AM, Watson D, Piersma SR, Jimenez CR, Luirink J, Bitter W, Houben EN. Specific chaperones for the type VII protein secretion pathway. J Biol Chem. 2012c; 287:31939–31947. [PubMed: 22843727]

Ekiert DC, Cox JS. Structure of a PE-PPE-EspG complex from Mycobacterium tuberculosis reveals molecular specificity of ESX protein secretion. Proc Natl Acad Sci U S A. 2014; 111:14758–14763. [PubMed: 25275011]

Emsley P, Lohkamp B, Scott WG, Cowtan K. Features and development of Coot. Acta Crystallogr D Biol Crystallogr. 2010; 66:486–501. [PubMed: 20383002]

Gey van Pittius NC, Sampson SL, Lee H, Kim Y, van Helden PD, Warren RM. Evolution and expansion of the *Mycobacterium tuberculosis* PE and PPE multigene families and their association with the duplication of the ESAT-6 (*esx*) gene cluster regions. BMC evolutionary biology. 2006; 6:95. [PubMed: 17105670]

Guinn KM, Hickey MJ, Mathur SK, Zakel KL, Grotzke JE, Lewinsohn DM, Smith S, Sherman DR. Individual RD1-region genes are required for export of ESAT-6/CFP-10 and for virulence of *Mycobacterium tuberculosis*. Mol Microbiol. 2004; 51:359–370. [PubMed: 14756778]

Houben D, Demangel C, van Ingen J, Perez J, Baldeon L, Abdallah AM, Caleechurn L, Bottai D, van Zon M, de Punder K, van der Laan T, Kant A, Bossers-de Vries R, Willemsen P, Bitter W, van Soolingen D, Brosch R, van der Wel N, Peters PJ. ESX-1-mediated translocation to the cytosol

controls virulence of mycobacteria. Cellular microbiology. 2012; 14:1287–1298. [PubMed: 22524898]

Houben EN, Korotkov KV, Bitter W. Take five - Type VII secretion systems of Mycobacteria. Biochim Biophys Acta. 2014; 1843:1707–1716. [PubMed: 24263244]

Ilghari D, Lightbody KL, Veverka V, Waters LC, Muskett FW, Renshaw PS, Carr MD. Solution structure of the Mycobacterium tuberculosis EsxG.EsxH complex: functional implications and comparisons with other M. tuberculosis Esx family complexes. J Biol Chem. 2011; 286:29993–30002. [PubMed: 21730061]

Kabsch W. Xds. Acta Crystallogr D Biol Crystallogr. 2010; 66:125–132. [PubMed: 20124692]

Korotkova N, Freire D, Phan TH, Ummels R, Creekmore CC, Evans TJ, Wilmanns M, Bitter W, Parret AH, Houben EN, Korotkov KV. Structure of the Mycobacterium tuberculosis type VII secretion system chaperone EspG in complex with PE25-PPE41 dimer. Mol Microbiol. 2014

Krissinel E, Henrick K. Secondary-structure matching (SSM), a new tool for fast protein structure alignment in three dimensions. Acta Crystallogr D Biol Crystallogr. 2004; 60:2256–2268. [PubMed: 15572779]

Langer G, Cohen SX, Lamzin VS, Perrakis A. Automated macromolecular model building for X-ray crystallography using ARP/wARP version 7. Nat Protoc. 2008; 3:1171–1179. [PubMed: 18600222]

Majlessi L, Brodin P, Brosch R, Rojas MJ, Khun H, Huerre M, Cole ST, Leclerc C. Influence of ESAT-6 secretion system 1 (RD1) of Mycobacterium tuberculosis on the interaction between mycobacteria and the host immune system. J Immunol. 2005; 174:3570–3579. [PubMed: 15749894]

McCoy AJ, Grosse-Kunstleve RW, Adams PD, Winn MD, Storoni LC, Read RJ. Phaser crystallographic software. J Appl Crystallogr. 2007; 40:658–674. [PubMed: 19461840]

McLaughlin B, Chon JS, MacGurn JA, Carlsson F, Cheng TL, Cox JS, Brown EJ. A mycobacterium ESX-1-secreted virulence factor with unique requirements for export. PLoS Pathog. 2007; 3:e105. [PubMed: 17676952]

Mishra KC, de Chastellier C, Narayana Y, Bifani P, Brown AK, Besra GS, Katoch VM, Joshi B, Balaji KN, Kremer L. Functional role of the PE domain and immunogenicity of the *Mycobacterium tuberculosis* triacylglycerol hydrolase LipY. Infect Immun. 2008; 76:127–140. [PubMed: 17938218]

Murshudov GN, Skubak P, Lebedev AA, Pannu NS, Steiner RA, Nicholls RA, Winn MD, Long F, Vagin AA. REFMAC5 for the refinement of macromolecular crystal structures. Acta Crystallogr D Biol Crystallogr. 2011; 67:355–367. [PubMed: 21460454]

O'Maille PE, Tsai MD, Greenhagen BT, Chappell J, Noel JP. Gene library synthesis by structure-based combinatorial protein engineering. Methods Enzymol. 2004; 388:75–91. [PubMed: 15289063]

Ohol YM, Goetz DH, Chan K, Shiloh MU, Craik CS, Cox JS. Mycobacterium tuberculosis MycP1 protease plays a dual role in regulation of ESX-1 secretion and virulence. Cell Host Microbe. 2010; 7:210–220. [PubMed: 20227664]

Painter J, Merritt EA. Optimal description of a protein structure in terms of multiple groups undergoing TLS motion. Acta Crystallogr D Biol Crystallogr. 2006; 62:439–450. [PubMed: 16552146]

Pallen MJ. The ESAT-6/WXG100 superfamily -- and a new Gram-positive secretion system? Trends Microbiol. 2002; 10:209–212. [PubMed: 11973144]

Poulsen C, Panjikar S, Holton SJ, Wilmanns M, Song YH. WXG100 protein superfamily consists of three subfamilies and exhibits an alpha-helical C-terminal conserved residue pattern. PLoS One. 2014; 9:e89313. [PubMed: 24586681]

Renshaw PS, Lightbody KL, Veverka V, Muskett FW, Kelly G, Frenkiel TA, Gordon SV, Hewinson RG, Burke B, Norman J, Williamson RA, Carr MD. Structure and function of the complex formed by the tuberculosis virulence factors CFP-10 and ESAT-6. EMBO J. 2005; 24:2491–2498. [PubMed: 15973432]

Robert X, Gouet P. Deciphering key features in protein structures with the new ENDscript server. Nucleic Acids Res. 2014; 42:W320–324. [PubMed: 24753421]

Serafini A, Boldrin F, Palu G, Manganelli R. Characterization of a *Mycobacterium tuberculosis* ESX-3 conditional mutant: essentiality and rescue by iron and zinc. J Bacteriol. 2009; 191:6340–6344. [PubMed: 19684129]

Siegrist MS, Unnikrishnan M, McConnell MJ, Borowsky M, Cheng TY, Siddiqi N, Fortune SM, Moody DB, Rubin EJ. Mycobacterial Esx-3 is required for mycobactin-mediated iron acquisition. Proc Natl Acad Sci U S A. 2009; 106:18792–18797. [PubMed: 19846780]

Siegrist MS, Steigedal M, Ahmad R, Mehra A, Dragset MS, Schuster BM, Philips JA, Carr SA, Rubin EJ. Mycobacterial Esx-3 requires multiple components for iron acquisition. mBio. 2014; 5:e01073–01014. [PubMed: 24803520]

Simeone R, Bobard A, Lippmann J, Bitter W, Majlessi L, Brosch R, Enninga J. Phagosomal rupture by *Mycobacterium tuberculosis* results in toxicity and host cell death. PLoS Pathog. 2012; 8:e1002507. [PubMed: 22319448]

Solomonson M, Huesgen PF, Wasney GA, Watanabe N, Gruninger RJ, Prehna G, Overall CM, Strynadka NC. Structure of the Mycosin-1 Protease from the Mycobacterial ESX-1 Protein Type VII Secretion System. J Biol Chem. 2013; 288:17782–17790. [PubMed: 23620593]

Solomonson M, Setiaputra D, Makepeace KA, Lameignere E, Petrotchenko EV, Conrady DG, Bergeron JR, Vuckovic M, DiMaio F, Borchers CH, Yip CK, Strynadka NC. Structure of EspB from the ESX-1 type VII secretion system and insights into its export mechanism. Structure. 2015; 23:571–583. [PubMed: 25684576]

Stanley SA, Raghavan S, Hwang WW, Cox JS. Acute infection and macrophage subversion by *Mycobacterium tuberculosis* require a specialized secretion system. Proc Natl Acad Sci U S A. 2003; 100:13001–13006. [PubMed: 14557536]

Strong M, Sawaya MR, Wang S, Phillips M, Cascio D, Eisenberg D. Toward the structural genomics of complexes: crystal structure of a PE/PPE protein complex from *Mycobacterium tuberculosis*. Proc Natl Acad Sci U S A. 2006; 103:8060–8065. [PubMed: 16690741]

Sultana R, Tanneeru K, Guruprasad L. The PE-PPE domain in mycobacterium reveals a serine alpha/beta hydrolase fold and function: an *in-silico* analysis. PLoS One. 2011; 6:e16745. [PubMed: 21347309]

Sultana R, Vemula MH, Banerjee S, Guruprasad L. The PE16 (Rv1430) of *Mycobacterium tuberculosis* is an esterase belonging to serine hydrolase superfamily of proteins. PLoS One. 2013; 8:e55320. [PubMed: 23383323]

Ummels R, Abdallah AM, Kuiper V, Aajoud A, Sparrius M, Naeem R, Spaink HP, van Soolingen D, Pain A, Bitter W. Identification of a novel conjugative plasmid in mycobacteria that requires both type IV and type VII secretion. mBio. 2014; 5:e01744–01714. [PubMed: 25249284]

van der Wel N, Hava D, Houben D, Fluitsma D, van Zon M, Pierson J, Brenner M, Peters PJ. *M. tuberculosis* and *M. leprae* translocate from the phagolysosome to the cytosol in myeloid cells. Cell. 2007; 129:1287–1298. [PubMed: 17604718]

Wagner JM, Evans TJ, Chen J, Zhu H, Houben ENG, Bitter W, Korotkov KV. Understanding specificity of the mycosin proteases in ESX/type VII secretion by structural and functional analysis. J Struct Biol. 2013; 184:115–128. [PubMed: 24113528]

Xu J, Laine O, Masciocchi M, Manoranjan J, Smith J, Du SJ, Edwards N, Zhu X, Fenselau C, Gao LY. A unique Mycobacterium ESX-1 protein co-secretes with CFP-10/ESAT-6 and is necessary for inhibiting phagosome maturation. Mol Microbiol. 2007; 66:787–800. [PubMed: 17908204]

Zhang KY, Cowtan K, Main P. Combining constraints for electron-density modification. Methods Enzymol. 1997; 277:53–64. [PubMed: 18488305]

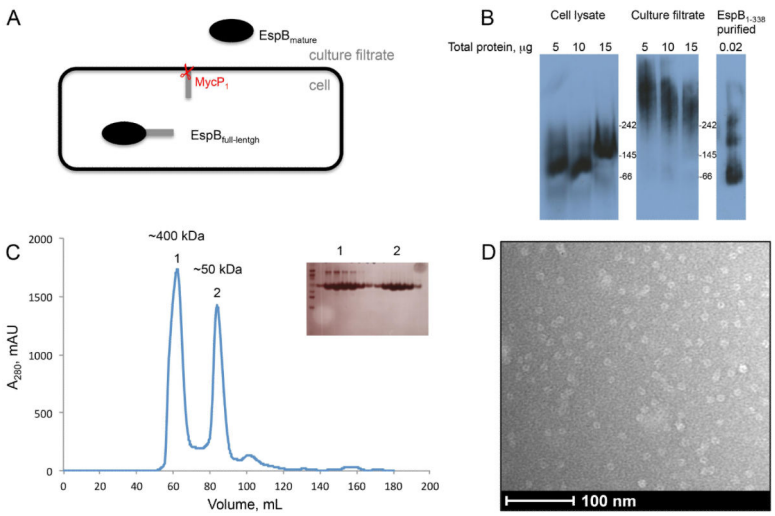

Fig. 1.

Oligomeric state of EspB.

A. EspB secretion model. The full-length protein (460 amino acids) is organized in two domains. The N-terminal domain belongs to the PE–PPE family and the C-terminal domain is predicted to be intrinsically disordered. The N-terminal fragment of EspB is secreted in the culture filtrate as the mature form after the cleavage by the serine protease $MycP_1$ (McLaughlin et al., 2007; Xu et al., 2007; Ohol et al., 2010).

B. Immuno-blotting of a native gel with different concentrations of cell lysate, culture filtrate of *M. tuberculosis* and purified $EspB_{1\text{-}338}$. Positions of molecular weight markers (kDa) are indicated.

C. Size exclusion chromatography profile of purified $EspB_{1\text{-}338}$ in 20mM Tris pH 8.5, 150 mM NaCl. Insert shows an SDS-PAGE of the peak fractions. The approximate size of oligomers (1) and monomers (2) were calculated by linear extrapolation.

D. Electron microscopy image of negative-stained $EspB_{1\text{-}338}$.

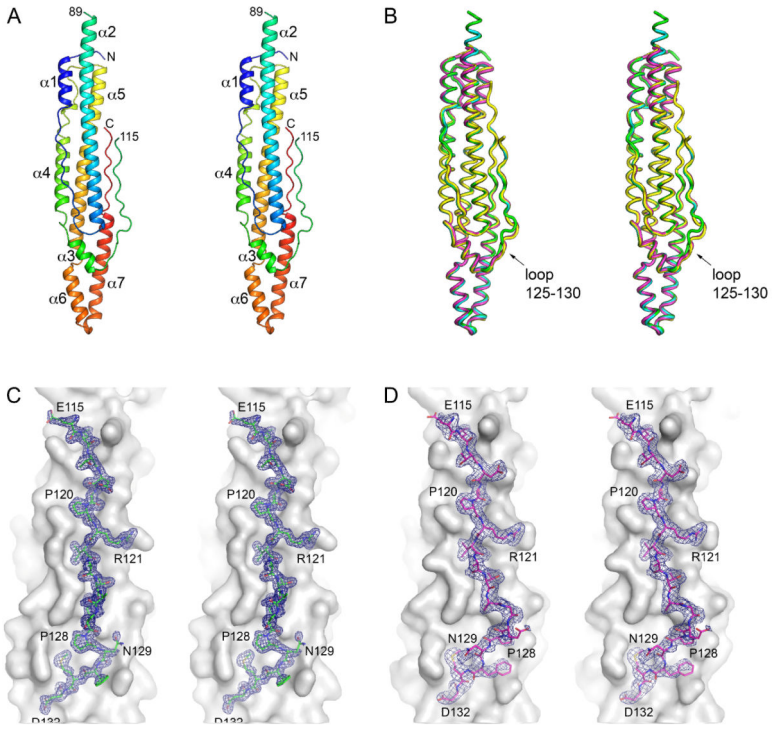

Fig. 2.

Structure of *M. tuberculosis* EspB.

A. A stereo view of $EspB_{7\text{-}278}$ structure (PDB: 4XXX) in cartoon representation colored in rainbow colors from the N-terminus (blue) to the C-terminus (red). The loop between helices α2 and α3 that connects PE and PPE domains of EspB is partially disordered (residues 90–114).

B. A stereo view of superposition of available EspB structures in ribbon representation. Cyan: $EspB_{7\text{-}278}$ in space group $C222_1$ (PDB: 4XWP); green: high-resolution structure of $EspB_{7\text{-}278}$ in space group $C222_1$ (PDB: 4XXX); magenta: $EspB_{7\text{-}278}$ in space group $I222$ (PDB: 4XXN); yellow: $EspB_{1\text{-}460}$ (PDB: 4XY3). The C-terminal domain of full-length $EspB_{1\text{-}460}$ is disordered. All structures are similar with the largest deviations found in the PE–PPE loop (residues 125–130). Structures were aligned using least-squares (LSQ) superposition in Coot (Emsley et al., 2010).

C and D. Stereo views of PE–PPE loop in $EspB_{7\text{-}278}$ structure in space group $C222_1$ (PDB: 4XXX) – (C) and in $EspB_{7\text{-}278}$ structure in space group $I222$ (PDB: 4XXN) – (D). Residues 115–132 are shown in stick representation with σA-weighted $2F_O\text{-}F_C$ electron density map contoured at 1σ. The rest of protein is shown as grey surface.

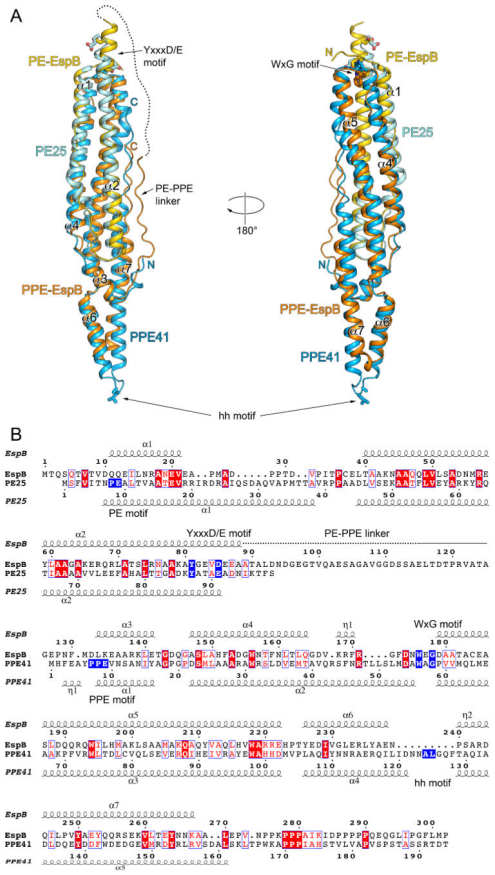

Fig. 3.

Comparison of EspB and PE25–PPE41 structures.

A. Structural superposition of $EspB_{7\text{-}278}$ (PDB: 4XXX) and PE25–PPE41 dimer (PDB: 4KXR). PE domain of EspB is in yellow; PPE domain of EspB is in orange; PE25 is in cyan; PPE41 is in light blue. The disordered region of PE–PPE linker of EspB is indicated by a dashed line. The secondary structure elements of EspB are labeled. The hh motif residues of PPE41, and the YxxxD/E motif residues of EspB and PE25 are shown in stick representation. Structures were superimposed using Secondary Structure Matching (SSM) (Krissinel and Henrick, 2004) as implemented in Coot (Emsley et al., 2010).

B. Structure-based sequence alignment of EspB and PE25–PPE41 based on superposition in (A). Secondary structure elements of $EspB_{7\text{-}278}$ and PE25–PPE41 are displayed above and below sequences, respectively. The characteristic sequence motifs of EspB and PE25–PPE41 are highlighted in blue. The alignment figure was generated using the ESPript 3.0 server (http://espript.ibcp.fr/ESPript/ESPript/) (Robert and Gouet, 2014).

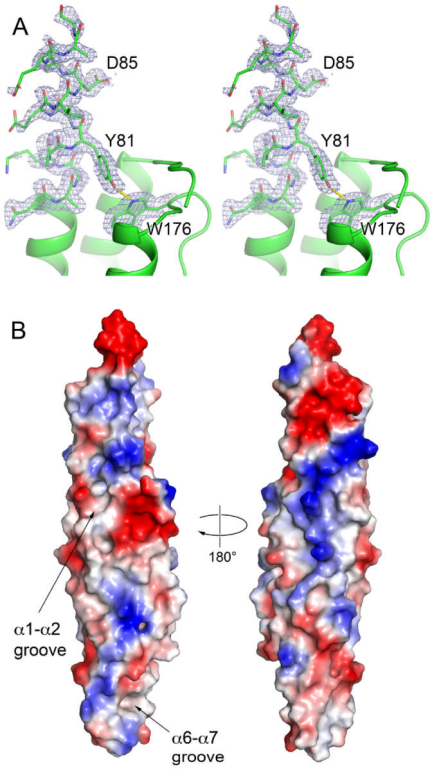

Fig. 4.

The YxxxD/E secretion motif and surface features of EspB.

A. Stereo views of YxxxD/E motif of $EspB_{7\text{-}278}$ (PDB: 4XXX). Residues 76–89 and W176 are shown in stick representation with sA-weighted $2F_O$-F_C electron density map contoured at 1σ. The rest of protein is shown in cartoon representation.

B. Representation of surface charge distribution of $EspB_{7\text{-}278}$ generated using PyMol. The putative lipid-binding sites of EspB are indicated.

Table 1

Data collection and refinement statistics.

	$EspB_{7-278}$ (PDB: 4XWP)	$EspB_{7-278}$ (PDB: 4XXX)	$EspB_{7-278}$ (PDB: 4XXN)	$EspB_{1-460}$ (PDB: 4XY3)
Data collection				
Space group	$C222_1$	$C222_1$	$I222$	$C222_1$
Cell dimensions □□				
a, *b*, *c* (Å)	66.24, 69.51, 119.14	67.34, 69.58, 119.60	73.12, 93.07, 142.94	72.11, 146.49, 94.22
α□ β□ γ□ (°)	90, 90, 90	90, 90, 90	90, 90, 90	90, 90, 90
Resolution (Å)	59.6–1.82 (1.92–2.00)[1]	59.8–1.50 (1.58–1.50)	71.5–2.14 (2.26–2.14)	47.11–3.04 (3.20–3.04)
R_{sym}	0.060 (0.945)	0.047 (0.747)	0.092 (0.873)	0.135 (0.917)
$CC_{1/2}$[2]	99.9 (86.3)	100.0 (88.4)	99.7 (54.1)	
$I / \sigma I$	17.8 (2.4)	18.6 (2.0)	13.8 (2.83)	9.0 (1.73)
Completeness (%)	100.0 (100.0)	99.7 (98.3)	97.8 (98.7)	95.7 (97.5)
Multiplicity	6.9 (7.0)	5.4 (5.1)	5.4 (5.5)	5.1 (5.1)
Refinement				
Resolution (Å)	59.6–1.82	59.8–1.50	71.5–2.14	47.11–3.04
No. reflections (total / free)	25047 / 1264	44892 / 2191	26733 / 1385	9490 / 491
R_{work} / R_{free}	0.199 / 0.234	0.194 / 0.218	0.204 / 0.251	0.220 / 0.266
No. atoms				
Protein	1863	1972	1875	1903
Ligand/ion	1	13	2	0
Water	159	263	174	0
B-factors				
Protein	37.6	27.2	45.6	82.5
Ligand/ion	56.8	36.0	50.8	
Water	43.4	36.5	46.6	
Wilson *B*	37.2	27.6	40.8	63.0
R.m.s. deviations				
Bond lengths (Å)	0.009	0.014	0.010	0.008
Bond angles (°)	1.228	1.518	1.312	1.220
Ramachandran distribution (%)[3]				
Favored	100.0	100.0	98.7	94.6
Outliers	0.0	0.0	0.0	0.8

[1] Values in parentheses are for the highest-resolution shell.

[2] Half-set correlation coefficient CC1/2 as defined in Karplus and Diederichs (Karplus and Diederichs, 2012) and calculated using XSCALE (Kabsch, 2010) or Scala (Evans, 2006).

[3] Calculated using the MolProbity server (http://molprobity.biochem.duke.edu) (Chen et al., 2010).